

Design and Analysis of Turbocharger Casing using CFD

Amruta R. Tonape¹, Prof. Dr.S.G.Arvindkumar²

¹PG Student, Department of Mechanical Engineering, Sanjeevan Engineering & Technology Institute, Kolhapur, Panhala, India.

²Assosiant Professor, Department of Mechanical Engineering, Sanjeevan Engineering & Technology Institute, Panhala, Kolhapur, India.

Abstract - A turbocharger turbine aids in extracting greater power from an I.C. engine. Exhaust gases from the I.C. engine are used to power the compressor via the turbocharger's turbine. In some circumstances, the failure of the turbine wheel blades is attributed to excessive cycle fatigue (HCF). To lessen the danger of failure, the last quadrant of the turbine housing is modified using the Creo-parametric tool and the sculptor tool. ANSYS CFX is used to calculate the pressure distributions in the turbine housing before and after the modification. This paper contains a way for lowering the Fourier amplitudes of this pressure distribution in order to lessen the probability of HCF failure. The final quadrant modification angle is seen to be dependent on static pressure distribution on the wheel perimeter and working critical orders, based on the findings of three turbine frames. In general, the region between 345 to 360 degrees is used to lower the Fourier amplitudes of critical orders 6 to 10. The turbine housing's tongue provides a wake region and non-uniformity, increasing the magnitude of pressure fluctuations on the wheel's periphery. If these Fourier amplitudes are large during resonance operation, the risks of wheel blade failure owing to HCF are considerable. Therefore, to reduce the risk of this HCF, the tongue can be moved away from the perimeter of the wheel. It can be seen that the rate of decrease in Fourier amplitude (to reduce the risk of turbine wheel blade failure) is about the same for large, medium and small turbine frames.

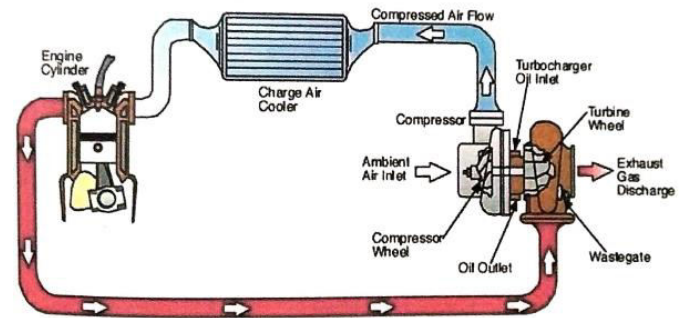


Figure 1: Schematic diagram of turbocharger on engine

Because the compressor is connected to the same shaft as the turbine wheel. The compressor's impeller draws in ambient air and transfers it to the IC engine. Because compressed air has a high temperature, the density of gas after compression is low. An intercooler is installed between the engine and the compressor to make the air denser.

Key Words: Turbocharger Turbine, Fourier analysis, CFD analysis, High Cycle Fatigue (HCF) failure, Turbine efficiency.

1. INTRODUCTION

A turbocharger is a turbine-powered forced induction device that boosts the efficiency and power output of an internal combustion (IC) engine by forcing additional compressed air into the combustion chamber. This increase in power production over a normally aspirated engine is due to the compressor's ability to drive more air and proportionally more fuel into the combustion chamber than ambient pressure alone[1]. Figure 1.1 displays the turbocharger's schematic diagram and operation. Exhaust gases from an IC engine have a high temperature and pressure after the exhaust stroke. This energy is used to power the turbine wheel as well as to recover energy from exhaust gases.

2. MAIN COMPONENTS OF TURBINE

It is worth noting that the outside cover of the turbine is referred to as the "housing," whereas the exterior cover of the compressor is referred to as the "cover." This terminology is used across the turbocharger business.

Turbine consists of

- Turbine housing /volute
- Wheel
- Diffuser

Turbine housing /volute: Turbine housing design changes change the performance of engine inlet and outlet conditions and space limiting requirements (i.e., mass flow rate, efficiency, turning angle, etc.). The design is chosen so that the pressure inside the turbine housing gradually decreases, as shown in Figure 1.2. The basic design requirements for bladeless turbine casings are,

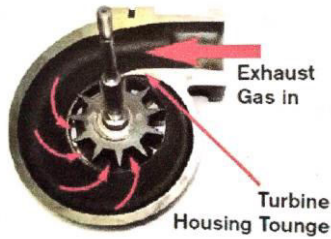


Figure 2: Turbocharger Turbine Cross-Sectional View

- It should provide a smooth flow around the periphery of the wheel.
- It should accelerate the working fluid to get the desired speed in the wheel in terms of size and direction for the resulting speed vector.
- The pressure and temperature distribution of exhaust gas around the wheels should be uniform.

Wheel: A combination of an induction hardened turbine wheel and shaft in the bearing journal for wear purposes is called a "turbine wheel". This is technically an assembly, but it can be called a separate part.

Diffuser: The part gradually expands from the wheel outlet to the exhaust pipe. After the exhaust gas is expanded by the turbine wheel, the pressure drop is almost lower than the atmospheric pressure. Therefore, the pressure is increased to release these gases for post-processing purposes and leave them free in the atmospheric diffuser. The diverging shape of the diffuser helps to increase its static pressure at the expense of speed. Generally, this increase in static pressure is also referred to as "pressure recovery".

3. LITERATURE REVIEW

The turbocharger turbine is used to extract energy from the exhaust gas discharged from the internal combustion engine and helps drive the compressor wheel/impeller. The proper design of the turbine stage has been tested for excellent performance and in some cases there has been a sudden failure of the wheel blades. In order to analyze this sudden impeller blade failure, some new analysis techniques and methods of modifying geometric shapes have been adopted. The computational fluid dynamics (CFD) research was also used. Methods of grid construction and its dependence on CFD results are important. Thus, a literature review is carried out on the above topics.

Kartik and Gautam [2] reviewed the turbocharger and supercharger. Here, they demonstrated the main advantages of combining turbochargers and superchargers with engines. Describes the

application/installation of turbochargers and superchargers. Kartik and Gautam[2] reviewed the turbocharger and supercharger. Here, they demonstrated the main advantages of combining turbochargers and superchargers with engines. Describes the application/installation of turbochargers and superchargers. Bhadi et al. [3] A brief overview of recent research and studies on turbine blade failure. After adopting several methods and techniques, they concluded that turbine blades mostly fail due to high cycle fatigue (HCF). Gunaki et.al.[4] conducted a structural analysis of the turbocharger turbine. The various factors of wheel failure are explained and the materials are optimized. Many new materials and composites have been tested on different components. Ibaraki et al.[3] carried out experimental and computational studies of the turbine housing. The two different trapezoidal cross-sectional shapes of the volute are modeled and the operating parameters under pressure pulsation conditions are analyzed. Arif et al.[5] the structural analysis of turbocharger turbine blades was carried out using structural steel. Heuer et al. [6] A study was conducted based on the effect of tongue design on turbine performance. It was concluded that the shape of the tongue affects the flow conditions at the wheel inlet. Ideally, the tongue should conform to the shape, but this is not possible from a production point of view. Darus et al. [7] A study on the heat distribution of the turbocharger turbine volute was presented.

Investigate the effect of the last quadrant change on Fourier amplitude and turbine performance.

Minimize the Fourier amplitude of the turbine housing by changing the last quadrant so as not to affect the performance of the turbine stage. (Sculptor tool)

Minimize the Fourier amplitude of the turbine housing by changing the tongue radius, so as not to affect the performance of the turbine stage. (Creo-paramatic tool)

To document the methods and result.

3.1 Turbine materials

The most commonly used turbine materials and sustainable temperature, Explains the different types of mesh methods for meshing the fluid domain of a turbine, out of which the robust octree method is explained in detail. Describes the Fourier series and Fourier transform of single / waveform theory. This is useful for analyzing the static pressure distribution around the turbine wheel.

Many materials are available for turbine housings and wheels. Some maximum temperature limits for materials are shown in Table 3.1 and Table 3.2.

Table 3.1: Housing material vs. Maximum allowable temperature

Material	Maximum allowable temperature(°C)
Ductile cast iron	700
Ductile cast iron alloy (SiMo)	780
Ferritic cast steel	950
Austenitic stainless cast steel	1100

Ductile iron (also known as ductile iron, nodular iron, spheroidal graphite iron, and circular iron and SG iron) is one of the most common materials used in this application. Ductile cast iron for exhaust gas applications, by itself, provides adequate strength for material temperatures of approximately 700oC. By increasing the content of silicon and molybdenum in the alloy, its heat resistance and high temperature strength can be increased, and the maximum material temperature can be raised to about 780oC. Ferritic cast steels and austenitic stainless steels can with stand temperatures of 950oC and 1100oC, respectively.

Table 3.2: Turbine wheel vs. maximum allowable temperature

Material	Maximum allowable temperature (°C)
$\gamma - T_iAl$	850
Inconel 713C	950
Mar-M-247	1050

A series of titanium-based alloys, gamma titanium aluminide ($\gamma - T_iAl$), may also be used in turbine wheels. This class of metal is significantly less dense than the Inconel 713C and Mar-M-247. ($\gamma - T_iAl$) produces a low inertia turbine wheel that significantly reduces turbocharger lag, as shown in Figure 3.1. These ($\gamma - T_iAl$) alloys are made up of about 45-48% of the weight of Al and the proper balance is Ti. Other alloying elements such as Si and Nb can be used to increase oxidation resistance, and chromium can be used to improve ductility. SI can also increase creep strength. The maximum permissible temperature of ($\gamma - T_iAl$) is about 850oC.

The body of the paper consists of numbered sections that present the main findings. These sections should be organized to best present the material.

4. COMPUTATIONAL FLUID DYNAMIC (CFD) ANALYSIS

In the Fourier analysis, the influence of the turbine casing on the pressure around the wheel was determined. Once the static pressure distributions on the circumference of the wheel are obtained, they are divided into orders to represent / convert them in the frequency domain. This conversion is a time domain to frequency domain conversion for better analysis of the waveform. Critical orders that correspond to the natural frequency of the wheel can cause resonance conditions, so only these orders are considered to decrease the Fourier amplitude. To find out these important orders, all orders are plotted on a Campbell chart.

An important part of a turbine in Fourier analysis is the turbine housing because it is the source of the pressure change. For ease of analysis, cut only the hub in the cavity, not the entire wheel. There is no interface inside the cavity. Therefore, this is a single domain entity. Due to this simplicity, the computational time required for Fourier analysis is shorter than for stage (performance) analysis.

5. ANALYSIS OF TURBINE HOUSING

In step-by-step analysis, several parameters are determined, such as isentropic efficiency, mass flow parameter, velocity parameter. For analysis, the scene cavity is divided into three domain: 1) body domain 2)

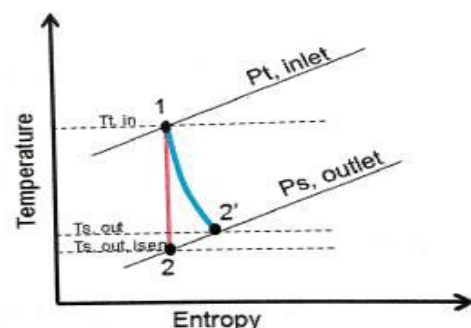


Figure 3: T-S diagram for turbine stage

wheel domain 3) diffuser domain. To achieve steady state conditions, the diffuser domain is sometimes extended by 1.5D. Where "D" is the diameter of the diffuser.

Some of the analytical relationships used to calculate the characteristics of the turbine housing are as follows:

In Figure 3, process 1-2 represents isentropic expansion, and 1-2' represents actual expansion.

Where, P_t = total pressure at inlet;

P_s = static pressure at outlet;

$T_{t, in}$ = total temperature at inlet;

$T_{s, out}$ = static temperature at outlet;

$t_{s, out, isen}$ = static isentropic temperature at outlet.

Note: For turbines, ER and efficiency are directly proportional to static conditions.

Expansion ratio [ER]

$$\frac{P_{t, inlet}}{P_{s, outlet}}$$

Where, P_t = total pressure at inlet; P_s = static pressure at outlet

Isentropic efficiency [η]:

$$\begin{aligned} &= \frac{W_{actual}}{W_{ideal}} \\ &= \frac{m C_p (T_1 - T_2)}{m C_p (T_1 - T_2')} \\ &= \frac{(T_1 - T_2')}{(T_1 - T_2)} \\ &= \frac{(T_1 - T_2')}{\left(T_1 \left(1 - \left(\frac{T_2}{T_1}\right)\right)\right)} \end{aligned}$$

We know, $(T_1/T_2) = (P_2/P_1)^{(\gamma - 1)/\gamma}$

$$\begin{aligned} &= \frac{(T_1 - T_2')}{T_1 \left(1 - \left(\frac{1}{ER}\right)^{\frac{\gamma - 1}{\gamma}}\right)} \\ &= \frac{(T_{t, in} - T_{s, out})}{T_{t, in} \left(1 - \left(\frac{1}{ER}\right)^{\frac{\gamma - 1}{\gamma}}\right)} \end{aligned}$$

Where, W = work done; C_p = specific heat at constant pressure; m = mass flow rate; γ = gamma.

Flow parameter [MFP]:

$$= \left((m * \sqrt{T_{inlet}}) / P_{inlet} \right)$$

Where m = mass flow rate; T = temperature at inlet; P = pressure at inlet.

CFD analysis is divided into 3 steps:

Pre-processing:

This preprocessing sets up geometry cleanup, meshing, and boundary conditions for analysis in ANSYS-CFX. The working fluid for analysis is the ideal air gas. Boundary conditions allow for the reproduction of truly functional behaviors. After the final configuration, the file is saved in def format for analysis.

5.1 Solver:

In this process, the actual analysis in CFX-SOLVER is performed using the CFD equations. The analysis is performed for a given number of iterations, and its convergence is verified by monitoring the inflow, outflow and imbalance plots. Convergence simply means that the difference between different iterations must be less than or equal to a given limit. Once convergence is reached, you can rely on the results.

5.2 Post-processing:

In this process, the extraction of results from the analysis is completed. Temperature distribution, pressure distribution, mass flow, etc. The various positions on the turbine casing help evaluate the performance of the turbine phase. Contour lines are plotted in different places for better representation / understanding. With continuous analysis, post-processing helps capture many of the changes that have occurred in the Fourier / turbine housing characteristics.

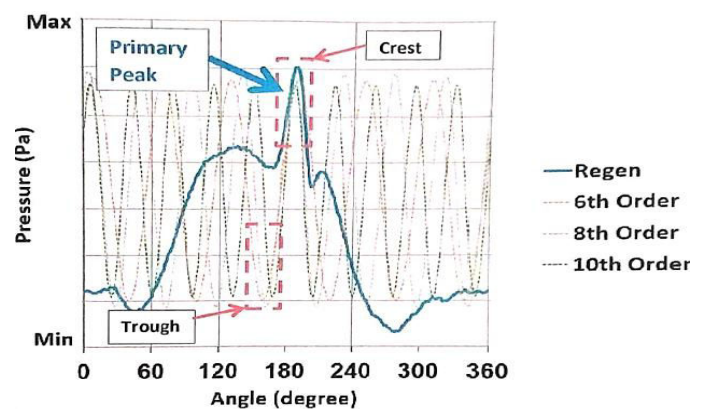


Figure 4: Static pressure distribution on wheel periphery

technique adopted to reduce the Fourier amplitude of critical working orders. This methodology is based on the waveform of the distribution of static pressure at the periphery of the wheel. This method is applicable to all three-turbine sizes (large, medium and small).

Figure 4 above shows the distribution of static pressure as a function of the angle of the base model. The regenerative wave shows the static pressure distribution around the wheel. The reconstructed signal is decomposed into sine and cosine signals using the

concept of a Fourier series, and only the order (critical order) is displayed on the reconstructed signal, the amplitude of which must be reduced.

According to the method we know, when two waves have the same side, they form a crest and when they are against each other (from time to time) they build a well.

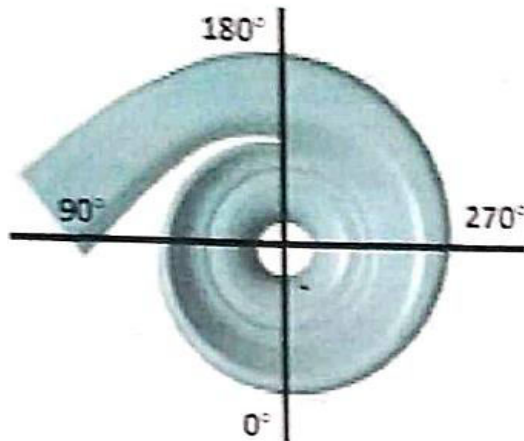


Figure 5: Static pressure distribution angle distribution

In Figure 5, the main peak is observed due to the tongue of the turbine housing. After this area of the tongue, the area suddenly increases and static pressure increases. Therefore, the peak is formed at about 180 degrees (tongue area). Critical working orders are observed to be nearly in phase with each other at the trough (near the tongue) just before the primary peak. Therefore, increasing the static pressure at this location will reduce the Fourier amplitude of the critical operating order. To understand the exact position and its effect on the Fourier amplitude, we made some geometric changes to the baseline geometry to create the concept. All of these concepts have a different deformation start angle, but the end angle remains the same.

5.3 Boundary Conditions for Numerical Analysis:

Describes the primary boundary conditions that are employed in the simulation to simulate the actual behavior of turbine housing. The baseline and changed geometry have the same requirements to capture the changes in modified geometry.

6. FOURIOUR AND STAGE ANALYSIS

The primary boundary conditions that are employed in the simulation to simulate the actual behavior of turbine housing. The baseline and changed geometry have the same requirements to capture the changes in modified geometry.

Table 8.1: boundary conditions for large size turbine

Conditions	Values
Turbulence model [Fourier]	k-epsilon
Turbulence model [stage]	SST
Working fluid	Air Ideal Gas
Turbine inlet gauge pressure (bar) [Fourier]	0.8,1.0,1.2,1.6,2.0
Turbine inlet gauge pressure (bar) [stage]	0.8,1.2,2.0
Turbine inlet temperature (K)	1136(863 ⁰ C)
Turbine outlet gauge pressure (bar)	0
Reference pressure (bar)	1

Table 8.2: working fluid properties for large size turbine

Thermodynamic state	Gas
Specific heat capacity	1168.698261[Jkg ⁻¹ K ⁻¹]
Transport properties	
Dynamic viscosity	Sutherlands formula
Ref. temperature	273.11[K]
Ref. viscosity	1.716e-05[Pa s]
Sutherland constant	110.56[K]
Temperature Exp.	1.5
Thermal conductivity	0.07491[W m ⁻¹ K ⁻¹]

Table 8.3: boundary conditions for medium and small size turbine

Conditions	Values
Turbulence model [Fourier]	k-epsilon
Turbulence model [stage]	SST
Working fluid	Air Ideal Gas
Turbine inlet gauge pressure (bar)	0.8,1.0,1.2,1.6,2.0

[Fourier]	
Turbine inlet gauge pressure (bar) [stage]	0.8,1.2,2.0
Turbine inlet temperature (K) [Fourier]	700(427 ⁰ C)
Turbine inlet temperature (K) [stage]	873(600 ⁰ C)
Turbine outlet gauge pressure (bar)	0
Reference pressure (bar)	1

Table 8.4: working fluid properties medium and small size turbine

Thermodynamic state	Gas
Specific heat capacity [Fourier]	1074.220557[Jkg ⁻¹ K ⁻¹]
Specific heat capacity [stage]	1114.965675[Jkg ⁻¹ K ⁻¹]
Transport properties	
Dynamic viscosity	Sutherlands formula
Ref. temperature	273.11[K]
Ref. viscosity	1.716e-05[Pa s]
Sutherland constant	110.56[K]
Temperature Exp.	1.5
Thermal conductivity [Fourier]	0.05230 [Wm ⁻¹ K ⁻¹]
Thermal conductivity [stage]	0.06161 [Wm ⁻¹ K ⁻¹]

As we know, in fourier analysis, a single domain entity is present, i.e., from the turbine inlet to the diffuser exit, only one fluid domain is there (no domain separation and absentism of the wheel), as illustrated in figures 8.1 (a), 8.2(c), and 8.3. (e). For stage analysis, the domain is divided into three subdomains (the presence of a wheel), so wheel rpm is also provided in table 8.5 for stage analysis to estimate turbine performance. Figures 8.1(b), 8.1(d), and 8.1(e) exhibit boundary conditions graphical

views for stage analysis of various turbine frame sizes (f).

When boundary conditions are imposed, Figure 8.1 displays the representation of stage and Fourier cavities.

Note:

- 1) There is no wheel in Fourier analysis.
- 2) A wheel is present in the stage analysis.

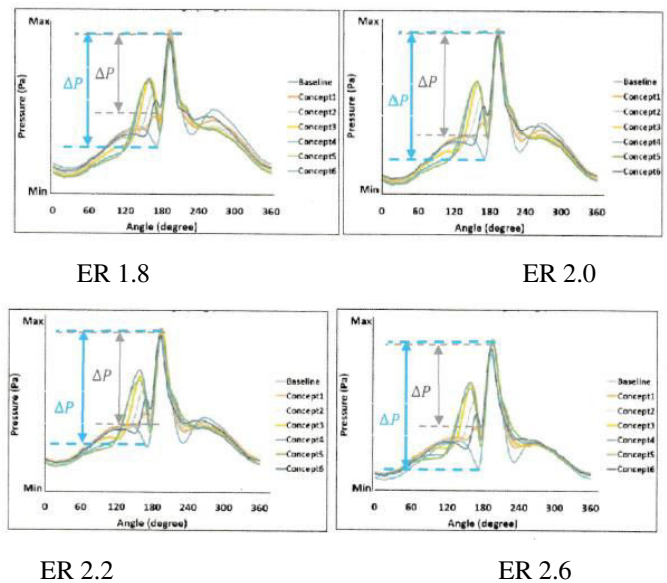
Table 8.5: wheel speed for stage analysis

Table 8.6 : solver controls

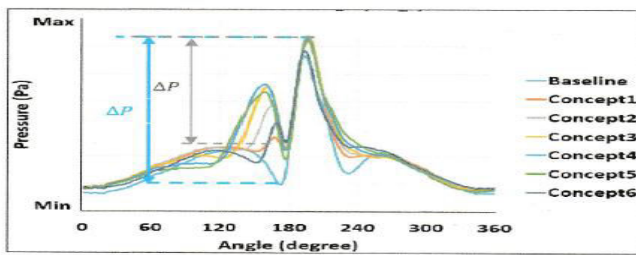
	ER 1.8	ER 2.2	ER 3.0
Large size turbine	62000 rpm	70000 rpm	82000 rpm
Medium size turbine	95000 rpm	108000 rpm	125000 rpm
Small size turbine	148000rpm	170000 rpm	197000 rpm

7. RESULTS AND DISCUSSION ON NUMERICAL ANALYSIS

CFD results are presented in this chapter, and they are discussed. Geometry overlay before and after alteration, area schedule before and after modification, static pressure distribution before and after modification, and the percentage variation in Fourier amplitude of critical operating orders are all shown. Because a large number of concepts were developed on the baseline geometry.



ER's	orders	Concept 1% diff	Concept 2% diff	Concept 3% diff	Concept 4% diff	Concept 5% diff	Concept 6% diff	Concept 7% diff
1.8	6	-24	-55	-77	-40	16	32	-10
	7	-15	-43	-57	-36	-5	-35	-49
	8	-25	-46	-38	8	0	-5	-32
	9	-15	-28	-20	-12	-7	-29	-7
	10	-23	-20	-4	23	-6	15	-1
2.0	6	-24	-55	-85	-11	44	45	-5
	7	-18	-46	-48	-22	10	-18	-46
	8	-23	-45	-46	-15	-16	-29	-47
	9	-16	-27	-11	8	3	-15	9
	10	-22	-25	-9	-5	-17	-11	-23
2.2	6	-3	-27	-61	-89	-42	-22	-36
	7	-33	-48	-21	16	26	-2	-7
	8	-18	-37	-34	-7	5	-19	-20
	9	-20	-38	-25	-1	-13	-29	-22
	10	-21	-11	13	11	-5	6	11



ER 3.0

Figure 6: Static pressure distribution (small size turbine)

8. CONCLUSIONS

High Fourier amplitude increases the likelihood of HCF failure in turbine wheels. To lessen the possibility of failure, the turbine housing's last quadrant was modified. These changes were performed utilizing both a traditional approach and a sculpting tool approach. The percentage drop in Fourier amplitude is roughly the same for big, medium, and small turbine frames.

The time required to implement each concept for last quadrant adjustment using the traditional approach is greater than that required using the sculptor tool approach. The wait time of the design department, as

well as the contact time between the design and analysis departments, played an important role in the old approach. The time consumed for last quadrant modification behind each concept is approximately 2 hours (30 minutes for modification using the creo tool + 1 hour 30 minutes for meshing in the ICEM CFD tool), with the use of the sculptor tool for last quadrant modification resulting in a significant time reduction. Because it features mesh morphing capabilities, the Sculptor tool approach takes only 30 minutes to generate the concept. The total time saved by each notion is 1 hour and 30 minutes, which is substantial.

Based on the results of three turbine frames, the final quadrant modification angle is found to be dependent on static pressure distribution on the wheel periphery and functioning critical orders. However, this region is generally taken from 345 to 360 degrees to reduce the Fourier amplitudes of crucial orders from 6 to 10.

The turbine housing's tongue provides a wake region and non-uniformity, increasing the magnitude of pressure variations on the wheel periphery. If these Fourier amplitudes are high during resonant operating conditions, the risks of wheel blade failure owing to HCF are considerable. To lessen the danger of HCF, the tongue part can be moved away from the wheel's periphery. The Fourier amplitude's magnitude is inversely proportional to the radius of the tongue.

REFERENCES

- [1] J. Galindo, S. Hoyas, P. Fajardo, and R. Navarro, "Set-up analysis and optimization of cfd simulations for radial turbines," *Eng Appl Comput Fluid Mech*, vol. 7, no. 4, pp. 441–460, 2013.
- [2] N. R. K. B.GAUTAM, "a Review on Turbocharger and Supercharger," *Int J Emerg Trends Eng Dev*, vol. 6, no. 5, 2016.
- [3] M. Yang, R. Martinez-Botas, S. Rajoo, T. Yokoyama, and S. Ibaraki, "An investigation of volute cross-sectional shape on turbocharger turbine under pulsating conditions in internal combustion engine," *Energy Convers Manag*, vol. 105, pp. 167–177, 2015.
- [4] A. R. Gunaki, "Analysis of Diesel Engine Turbocharger & its Optimization Akash Roopkumar Gunaki Department of Mechanical Engineering," vol. 5, no. 05, pp. 875–880, 2017.
- [5] R. Kalvin, A. Nadeem, and S. Arif, "Stress Analysis of Turbine Blades of Turbocharger Using Structural Steel," vol. 12, no. 9, pp. 929–932, 2018.
- [6] S. Matsuo, M. Mohammad, J. Nagao, T. Hashimoto, T. Setoguchi, and H. D. Kim, "Effect of non-equilibrium condensation in shear layer on supersonic impinging jets," *Procedia Eng*, vol. 56, pp. 437–444, 2013.
- [7] K. Kowsari, D. F. James, M. Papini, and J. K. Spelt, "The effects of dilute polymer solution elasticity and viscosity on abrasive slurry jet micro-machining of glass," *Wear*, vol. 309, no. 1–2, pp. 112–119, 2014.